

# Integrative Biology

Accepted Manuscript



This is an *Accepted Manuscript*, which has been through the Royal Society of Chemistry peer review process and has been accepted for publication.

*Accepted Manuscripts* are published online shortly after acceptance, before technical editing, formatting and proof reading. Using this free service, authors can make their results available to the community, in citable form, before we publish the edited article. We will replace this *Accepted Manuscript* with the edited and formatted *Advance Article* as soon as it is available.

You can find more information about *Accepted Manuscripts* in the [Information for Authors](#).

Please note that technical editing may introduce minor changes to the text and/or graphics, which may alter content. The journal's standard [Terms & Conditions](#) and the [Ethical guidelines](#) still apply. In no event shall the Royal Society of Chemistry be held responsible for any errors or omissions in this *Accepted Manuscript* or any consequences arising from the use of any information it contains.

# Modeling Type 2 Diabetes–like Hyperglycemia in *C.elegans* on a Microdevice

Guoli Zhu, Fangchao Yin, Li Wang, Wenbo Wei, Lei Jiang and Jianhua Qin\*

\*Laboratory of Biotechnology, Dalian Institute of Chemical Physics,  
Chinese Academy of Sciences, 457 Zhongshan Road, Dalian, 116023, China.  
E-mail: jhqin@dicp.ac.cn; Fax: +86-411-84379650

*Caenorhabditis elegans* (*C. elegans*) has been widely used as a model organism for biomedical research due to its sufficient homology with mammals at the molecular and genomic levels. In this work, we describe a microfluidic assay to model type 2 diabetes–like hyperglycemia in *C.elegans* to examine several aspects of this disease on a microdevice. The microdevice is characterized by the integration of long-term worm culture, worm immobilization, and precise chemical stimuli in a single device, thus enabling the multi-parameter analysis of individual worms at a single-animal resolution. With this device, the lifespan, oxidative stress responses, and lipid metabolism of individual worms in response to different glucose concentrations were characterized. It was found that the mean lifespan of worms was significantly reduced by as much as 29.0% and 30.8% in worms that were subjected to 100-mM and 200-mM glucose, respectively. The expression of oxidative stress protein *gst-4* was increased, and the expression of the *hsp-70* (heat shock protein) and *skn-1* (redox sensitive transcription factor) genes was down-regulated in worms treated with a high level of glucose. Moreover, fat storage was markedly increased in the bodies of VS29 worms (*vha-6p::GFP::dgat-2*) that were exposed to the high-glucose condition. The established approach is not only suitable for further elucidation of the mechanism of metabolism disorders involved in diabetes and its complications, but also facilitates the evaluation of anti-diabetes drugs in a high-throughput manner.

## Insight, innovation, integration

We described an integrated microfluidic device to model type 2 diabetes–like hyperglycemia in *C.elegans* and examine several aspects of this disease in *C.elegans* for the first time. The high-glucose condition was found to significantly shorten the lifespan of *C. elegans* with increased oxidative stress and lipid formation in transgenic *C.elegans*. These findings highlight the possible contribution of *C. elegans* to our understanding of diabetes in higher organisms. Moreover, this device is capable of flexible operation with individual worms and with multiple functions and can be easily applied for the study of diabetic complications and testing of medications to treat metabolism disorders.

## Introduction

*Caenorhabditis elegans* (*C. elegans*) is an invaluable model organism for biomedical

research because it can be used to recapitulate many aspects of human diseases at either the molecular or genomic level *in vivo*<sup>1,2</sup>. As the first animal whose genome was completely sequenced, *C. elegans* is more than 40% homologous to human genes that have been implicated in many human diseases. *C. elegans* is a small free-living soil nematode that is characterized by several unique features, such as its small size, short lifespan (2 to 3 weeks), ease of propagation, and optically transparent body. Significant progress has been made in the delineation of the genetic and biochemical pathways involved in human disorders with this model organism and in the identification of effective strategies for therapeutic intervention in humans<sup>3-6</sup>. In particular, this organism contains many key components related to the metabolism, oxidative stress network, and insulin-signaling pathway, making it a useful system to improve our understanding of complex diseases such as diabetes<sup>7,8</sup>.

Diabetes mellitus is a metabolic disorder that affects millions of people worldwide and contributes considerably to the global mortality rate<sup>9</sup>. It is characterized by poor control of glucose homeostasis. Glucose, as a major energy source and key regulator of metabolism, induces pancreatic  $\beta$ -cells to secrete insulin, which in turn facilitates the transport of glucose to tissues such as muscle and adipose<sup>10</sup>. However, a chronic overabundance of glucose or fructose will have deleterious effects on cellular and tissue functions and has been linked to several disorders including type 2 diabetes, obesity, and cardiac dysfunction<sup>11-13</sup>. *Schlotterer et al* reported that high glucose may shorten the lifespan of worms<sup>7</sup>, and the reduced lifespan was obtained by down regulating DAF-16/FOXO activity and aquaporin gene expression<sup>8</sup>. Recent studies have shown that glucose increases fat accumulation in mammals and in worms<sup>14,15</sup> and may affect the stress response<sup>10,13,16,17</sup>. Diverse studies have demonstrated that oxidative stress participates in the progression of diabetes complications<sup>18</sup>. Genes like *skn-1* and *hsp-70* were found to be the protective genes against oxidative stress<sup>[19-23]</sup>. Moreover, *sbp-1*, *nhr-49*, *fat-6* and *fgt-1* were the homologue genes with mammals which regulated the fat and glucose metabolism<sup>[24-28]</sup>. Although many advances have been made in our understanding of the pathophysiology of diabetes mellitus, its prevalence continues to increase, due in part to changes in lifestyle, increased overall life expectancy, and the complex regulation mechanism that underlies the pathologic process.

In the past few years, microfluidics technology has provided an attractive platform for the study of *C. elegans* due to its perfect dimension with the size of worms, flexible operation of precise stimuli, seamless integration of active control elements, and its capability for potential high-throughput analysis. Several channel-based and droplet-based microfluidic devices have been developed for various worm manipulations, including worm culture, immobilization, microsurgery, and neural imaging<sup>29-37</sup>. They have also been applied to exploit *C. elegans* as a suitable model for the study of neurobiology, development, Parkinson's disease, aging and behaviour<sup>34, 36, 38-42</sup>. However, no work has been devoted to the study of metabolism disorders relevant to diabetes in *C. elegans* on the microfluidic device.

In this study, we propose an integrated microfluidic device to resemble the hyperglycemic condition in diabetics using *C. elegans* as a model. We investigated the various responses of *C. elegans* exposed to a continuously high glucose concentration

in a physiologically relevant manner. The microfluidic device exhibits multiple functions by integrating long-term worm culture with individual worm manipulations in a high-throughput format at a single-animal resolution. We characterized the lifespan, oxidative stress, and lipid formation of *C.elegans* under a continuous high-glucose condition on the microdevice. We also evaluated the mRNA expression of genes associated with oxidative stress, glucose, and fat metabolism. The worms exhibited a shortened lifespan and increased oxidative stress and lipid formation after exposure to a high glucose concentration, indicating their relevance to the pathological changes that appear in patients with diabetes. These results demonstrate the utility of this microfluidic device for multi-parameter analysis of metabolic disorders in *C.elegans*, thus facilitating the exploration of the mechanism of metabolism disorders and effective evaluation of pharmaceutical compounds for the treatment of diabetes or its complications.

## Experimental

### 1. Fabrication of microfluidic device

As shown in Fig. 1, the design of the microfluidic device is based on our previous work with major modifications.<sup>38</sup> It mainly consists of a microfluidic network including a top worm culture layer and a bottom control layer. This device was fabricated using multilayer soft lithography and rapid prototyping techniques.<sup>43-46</sup> Briefly, Si wafers were patterned with SU-8 3035 photoresist (Microchem Corp, Newton, MA) and subjected to the photolithographic processes to achieve a mold with particular dimensions. To fabricate the culture chamber, polydimethylsiloxane (PDMS; Sylgard silicone elastomer 184, Dow Corning Corp., Midland, MI) at a 12:1 base-to-curing agent weight ratio were cast onto the flow layer wafer followed by degassing and curing at 80 °C for 1h. As for the control layer, after patterning, the masters were silanized by exposure to tridecafluoro-1,1,2,2-tetrahydrooctyl trichlorosilane vapor (Sigma Chemical) and positioned in Petri dishes<sup>43, 47</sup> to prevent the PDMS from adhering to the master. Then, 12:1 ratio PDMS was spun on the master, degassed under a vacuum, and cured (80 °C; 1h) to achieve a 40- $\mu$ m-thick membrane higher than the structure that is used to avoid the adhesion of PDMS and the substructure. The flow layer was peeled off the silicon wafer and bonded onto the control layer by plasma bonding. The assembly was gently peeled from the master and trimmed to size, and holes were punched (2-mm diameter). Finally, all devices were bonded onto a glass slide by plasma bonding.

The dimension of the microfluidic network was designed to meet the requirement of continuous worm analysis. In the top layer, the worm loading channel was gradually narrowed from 250  $\mu$ m to 30  $\mu$ m and lengthened to 1.5mm. The dimension of the culture chamber is 2mm long, 1.2mm wide, and 65  $\mu$ m tall, which is suitable for worm culturing and immobilization in the control layer. This design of micropillar structure is used for sorting L1-L2 worms to guarantee a single adult worm in the microchamber. The 30 filter channels are all linked to the central waste reservoir through a 20- $\mu$ m-wide

channel.

## 2. Worm culture and strains

*C. elegans* wild-type N2 and all transgenic strains in this study were obtained from the Caenorhabditis Genetics Center at the University of Minnesota–St. Paul. The transgenic strain CL2166 (*gst-4::GFP*) containing *gst-4* reporter was used to illustrate the inducible oxidative stress in the worms. The VS29 strain (*vha-6p::GFP::dgat-2*) was used to represent the expression quantity of lipid in the worms.

All strains were cultivated as described by Brenner<sup>3</sup>. Briefly, the worms were cultivated at 20 °C on standard nematode growth medium agar seeded with *Escherichia coli* OP50. Before seeding, the bacteria were incubated overnight at 37 °C and stored at 4 °C.

## 3. Worm synchronization

To synchronize the growth stage of the nematodes, adult worms were treated with NaClO solution 5M NaOH/NaClO/H<sub>2</sub>O(1:2:7) at room temperature until the skin of each individual was mostly destroyed.<sup>39</sup> The eggs were collected and cultured overnight on fresh nematode growth medium agar plates at 20 °C until hatching.

## 4. Glucose assays in worms

Different concentrations (0 mM, 100mM and 200mM) of glucose solution were obtained by diluting 40% D(+)-glucose (Sigma) to K medium (50 mM NaCl, 30 mM KCl, 10 mM NaOAc, pH 5.5). Age-synchronous wild-type N2 worms were hatched at the L1 stage and then transferred to microtiter plates and treated with a prepared glucose solution from the L1 stage, the medium was exchanged every day during the worms' lifetime. The worms were kept for 7 days under various glucose concentrations in the microtiter plates prepared as described above, harvested, and washed. An extract of worms was prepared by sonication and analyzed for glucose concentration using a glucose assay kit (Bioassay System).

## 5. Lifespan assays in worms

The microfluidic device was fabricated as described above, and the lifespan assays were performed at 20 °C. The hatched worms (L1 stage) were transferred to K medium in microtiter plates for treatment with glucose. The concentration of glucose was either 100mM or 200mM. The worms were then cultured at 20 °C with *E. coli* strain OP50 as a food source until they reached the L4 stage. The L4 worms were loaded into the microfluidic device. After the worms stabilized in the chambers, we treated them with food OP50 and glucose solution by exchanging the medium twice each day. Worms that did not move after repeated stimulus were regarded as dead. The lifespan assay was performed with a charge-couple device mounted on a stereozoom microscope (Leica S8APO, Germany). After the L4 worms were loaded into the chip, their survival activity was monitored daily.

## 6. Fluorescent microscope

The green fluorescence of CL2166 and VS29 worms was examined with an inverted fluorescent microscope (Olympus IX 71, Japan). The excitation and detection wavelengths were set at 470 to 495 nm and 510 to 550 nm, respectively. The fluorescence images were analyzed with image processing and analysis software (IMAGE-PRO, Media Cybernetics, USA) to determine their mean fluorescence density.

## 7. Quantitative real-time polymerase chain reaction

The mRNA expression of oxidative stress associated genes and lipid metabolism genes was assessed by means of a real-time quantitative polymerase chain reaction (PCR) system (Piko Real 2.1) using SYBR green(Takara) as the detection method. The L1 worms were treated with various concentrations of glucose for 72 h and grown until adult. The total RNA was then extracted from the adult worms according to the Trizol treatment procedure. cDNA was produced by oligo (dT) priming(Takara). PCR(95 °Cfor 30s; 40cycles of 95 °Cfor 5s, 57 °C for 30 s, 72 °C for 30s;60 °C to 95 °Cmelt curve) was performed using each primer(Table 1).act-1 was used as the internal control.

## 8. Statistical analysis

Statistical analysis was performed by applying a two-tailed Students't test to compare the high-glucose treated group and the non-treated group. The software Excel was used in this work.

# Results

## 1. Design and operation of microdevice

To explore the various effects of high glucose concentrations on *C. elegans* in a controllable manner, we used a microfluidic device made of an optically transparent PDMS silicone elastomer that contains a flow layer and a control layer, as shown in Fig.1A. The top layer includes 30 microchambers connected to the microchannel network for loading, culturing, and sorting of individual worms (Fig. 1B). The bottom layer is designed for immobilization of single worms via valve control for imaging analysis (Fig. 1C). The width of the loading channels was gradually reduced to facilitate the loading of individual worms into the culture microchamber for subsequent analysis. The micropillar structure connected to the microchamber is designed to filter out the tiny young L1 and L2 worms, while maintaining a single adult worm within each chamber during the loading and long-term culture process (Fig.1D).

Before the worm assays, single worms were loaded into the culture microchamber by pressure-driven flow via a central waste outlet. Once loaded, the worms were confined to the microchamber surrounded by long inlet channel and micropillars. To achieve long-term worm culture, the worms were infused with sufficient oxygen and food from the worm inlet to the culture chamber twice daily, while maintaining continuous expulsion of metabolites. Glucose was added by mixing it with the food solution and injecting it into the individual loading channels to maintain worm growth under the same glucose concentrations. To perform imaging analyses, the individual worms were



immobilized by deforming the membrane of the bottom layer using the microvalve control. The integrated microfluidic device enables worm loading, long-term culture with chemical stimuli, and immobilization with imaging analysis in parallel in a controllable manner, thus facilitating the multi-parameter analysis and real-time tracking of worms under different glucose conditions at single-animal resolution.

## **2. Dietary glucose triggered different responses in *C. elegans***

In this study, the intracellular glucose concentrations in worms were determined from whole-body extracts after culturing for 7 days in various glucose concentrations. Under glucose concentrations of 100mM and 200mM, the intracellular glucose concentrations from the body extracts of worms were measured at 6.7mM and 12mM, respectively, with a glucose assay kit. Because the measured value corresponds to the blood glucose range observed in patients with poorly controlled diabetes, we further characterized the effects of hyperglycemia on the lifespan, stress responses, and fat metabolism of *C.elegans* in the following experiment.

### **2.1 Effect of high glucose concentration on lifespan of *C.elegans***

To investigate whether glucose influenced the lifespan of wild-type N2 worms that are normally fed a diet of *E.coli* OP50 bacteria, the worm culture medium was added to food containing glucose on the microfluidic device. After synchronization, the worms were treated with various glucose concentrations (0mM, 100mM, and 200mM) at the L1 stage for 48h in a multiwell plate. After growth to adulthood, the individual worms at the L4 stage were picked randomly and loaded into the confined microchamber (defined as day 0). The glucose and a lawn of bacteria were added to the chamber and refreshed every day. Based on the design of the microchip, 30 worms could be individually treated, observed, and imaged in parallel. The wild-type N2 worms treated with various glucose concentrations exhibited different development processes in the device, and all worms were monitored for survival every day. Worms in the high-glucose condition grew older than those in the control group (Fig.2A). As shown in Fig.2B, the percentage of live worms was significantly higher in the normal culture than in the high-glucose condition spanning the developmental stages. The mean lifespan of N2 worms was 16.2 days under normal conditions, whereas it was shortened to 11.5 days and 11.2 days in 100mM and 200mM glucose (Fig.2C), respectively. The high glucose condition was found to significantly shorten the mean lifespan of worms by up to 29.0% and 30.8% in these two groups, indicating the influence of excess glucose intake on the worms' lifespan.

### **2.2 Effect of glucose on expressions of oxidative stress protein and associated genes**

Oxidative stresses derived from exogenous and endogenous substances are considered to cause cancer, inflammation, diabetes, and several age-related diseases.<sup>6, 32</sup> Oxidative stress is also recognized as an etiologic factor that influences numerous human diseases including diabetes. In this work, we made an attempt to explore the effect of a high-glucose condition on the oxidative stress responses in worms by characterizing the expression of inducible oxidative stress protein in transgenic worms (*gst-4::GFP*

nematodes CL2166). This transgenic strain is characterized by a fusion transgene in which the green fluorescent protein (GFP) is fused under the *gst-4* promoter. The fluorescence intensity of GFP expression in transgenic CL2166 worms was adopted to represent the induced oxidative stress level of the worms in response to different concentrations of glucose. The L1 worms pretreated with different glucose concentrations (0mM, 100mM, and 200mM) were divided into three groups and cultured to the L4 stage. The L4 worms were loaded and cultured in the microchamber and the medium exchanged each day.

As shown in Fig. 3A, we observed weak GFP expression in the *gst-4::GFP* worms under normal culture conditions. However, the inducible oxidative protein expression was increased significantly in the bodies of the *gst-4::GFP* worms after acute exposure to glucose. From the results in Fig. 3B, the protein expression level was significantly higher in the glucose-treated groups than in the control group. Moreover, the protein expression level was higher in the worms treated with 200mM glucose than in those treated with 100mM glucose, suggesting a dose-dependent response. Furthermore, the trend of *gst-4* protein expression in worms under various glucose concentrations over 7 days is shown in Fig. 3C. It was noted that the expression of GST-4 in the individual worms began to decrease at day 1 after glucose treatment; it continued to decrease at day 5 and became stable at day 7 in both treated and non-treated groups, indicating that the body's resistance to oxidative stress declined gradually as the body aged. Taken together, the data from these studies suggest that *gst-4* may be involved in the hermetic response to glucose and contributes to the worms' response to glucose exposure.

We further investigated the expression of the *hsp-70* and *skn-1* genes in wild-type N2 worms subjected to high glucose levels. As shown in Fig. 4, we observed less mRNA expression of *hsp-70* in glucose-treated worms than in untreated worms by quantitative real-time PCR analysis. The down-regulation of *hsp-70* suggests that it may be damaged under cellular stress caused by hyperglycemia. The mRNA expression of the *skn-1* gene was also down-regulated in worms subjected to a high glucose concentration compared to those in the normal culture condition, indicating the potential role of *skn-1* in protecting tissue against oxidative stress in high concentrations of glucose.

### 2.3 Effect of glucose on lipid formation and fat metabolism-associated genes

As stated above, because the worms exhibited a shortened lifespan and an increased oxidative stress level after exposure to a high glucose concentration, we further explored the possibility of glucose stimuli on the formation of lipid droplets and the expression of fat metabolism-related genes at mRNA levels. Because recent evidence suggests that DGAT2 may localize to lipid droplets upon lipid loading in mammalian cells<sup>48-50</sup>, we choose the transgenic strain worm VS29 (*hjsi56 vha-6p::GFP::dgat-2*) to study lipid droplet formation in worms under different conditions. The worms were pretreated with different glucose concentrations (100mM or 200mM) from the L1 stage. The fluorescence image of GFP expression in this transgenic strain was recorded on different days (1st, 3rd, 5th, and 7th days). Fig. 5A demonstrates the time-course fluorescence images of lipid storage in worms under different glucose concentrations. The mean relative fluorescence intensity represents the degree of lipid droplet



formation in worms subjected to different treatments. The quantitative results of GFP::dgat-2 expression in VS29 worms during the aging process is shown in Fig. 5B. In contrast to the control worms, the lipid storage in the individual worms began to increase at day 1 after glucose treatment; it continued to increase at day 5 and showed no obvious difference at day 7. However, we did not find a significant difference in lipid storage between the transgenic worms treated with 100-mM glucose and those treated with 200-mM glucose. Fig. 5C shows the trend of expression of GFP::dgat-2 in VS29 worms for glucose-treated worms compared to non-treated worms over 7 days. The relative expression of GFP::dgat-2 gradually reduced from the fifth day for the glucose-treated group, indicating that the capacity of lipid storage was weakened from the fifth day.

From the quantitative real-time PCR analysis shown in Fig. 6, the mRNA expression was remarkably increased in fat metabolism genes *sbp-1*, *nhr-49*, and *fat-6*. The *sbp-1* mRNA levels increased markedly, especially in the presence of glucose. The expression of glucose metabolism-related gene *fgt-1* was significantly reduced in worms subjected to high glucose conditions for 72h. These observations suggest that fat levels increase with the intake of excess calories from glucose in *C.elegans* just as they do in mammals. The profound increase of *sbp-1* and *nhr-49* at the mRNA level indicated that high glucose intake facilitated fat storage in the intestines of the worms. The transport of glucose from the intestinal cells of worms after high-glucose intake may be disturbed by down-regulation of *fgt-1*.

## Discussion

The main purpose of this study was to establish *C.elegans* as a model of type 2 diabetes for the study of metabolism disorders on a microdevice and facilitate our understanding of the possible mechanism that underlies the effects of glucose on lifespan, oxidative stress, and glucose/lipid metabolism in diabetes research. We characterized the lifespan, oxidative stress, and lipid storage of *C.elegans* under continuous high-glucose conditions on the microdevice. We found that long-lasting high-glucose conditions result in a significant reduction in lifespan, an increase in the oxidative stress level, and the accumulation of lipid storage in worms, reflecting the relevant pathological changes that appear in patients with diabetes. Because the total body glucose concentrations of 6.7mM and 12mM were sufficient to achieve significant effects on lifespan, oxidative stress, and fat storage, this in vivo model organism in the microdevice provides a potential platform with which to decipher the changes in lifespan, cellular functions, glucose, and fat metabolism disorders triggered by excess glucose intake that are within the range observed in patients with poorly controlled diabetes.

Several studies have addressed the effects of dietary glucose on obesity and diabetes, but little is known about its effect on the lifespan itself. We found that a diet of glucose shortened the lifespan of *C.elegans* by approximately 29.0% and 30.8% at the two difference concentrations. Because aging is the most important risk factor for many diseases, including diabetes and cancer, the discovery of effective modulators of lifespan in model organisms could promote new strategies for the treatment of diabetes and other aging-related diseases. In this work, the high-glucose condition was observed

to promote the increased expression of oxidative stress protein in transgenic CL2166(*gst-4::GFP*) strains. It also down-regulated the expression of the stress-associated *skn-1* and *hsp-70* gene at the mRNA level in wild-type N2 worms. These data are consistent with our previous findings that the lifespan of worms is closely associated with the oxidative stress induced by external stimuli.<sup>39</sup>

In mammals, several phase II enzymes, like GST, are regulated by the bZIP transcriptional factor Nrf2 in response to oxidative or electrophilic stresses.<sup>51</sup> In *C. elegans*, the transcription factor SKN-1 is found to have a function similar to that of Nrf2 by inducing GST-4 expression in response to oxidative stresses. It has been reported that *skn-1* may protect neighboring tissues from damage from oxidative stress<sup>21</sup> and that *skn-1* mutants are sensitive to oxidative stress and have shortened lifespans<sup>22</sup>. The *hsp-70* genes and humans have a high degree of homology and share a conserved core “adenosine triphosphatase” structure<sup>52</sup> and it is associated with cellular stress and may protect against obesity-associated insulin resistance<sup>23</sup>. Therefore, we assume that oxidative stress triggered by high levels of glucose may contribute to the shortened lifespan in worms and that this effect might be associated with the regulatory role of the *skn-1* gene. This also supports the notion that oxidative stress might cause a reduction in cellular adenosine triphosphate levels, thus leading to the continued prevention of the aggregation of damaged proteins.<sup>53</sup>

Diabetes is characterized by some critical features, including glucose and lipid metabolism disorders. Several genes have been revealed to regulate the glucose and lipid metabolism in vivo. It has been reported that *sbp-1*, as a homolog of the mammalian transcription factor SREBP-1c, can facilitate fat storage in mammals<sup>24</sup>. In addition, *nhr-49*, similar to the mammalian PPARs<sup>25</sup>, can modulate fat consumption and composition<sup>26</sup>. *fat-6*, encoding delta-9 desaturase for the synthesis of unsaturated fatty acids, was expressed in the intestine<sup>27</sup> and indicated fat storage. In contrast, the function of *fgt-1*, the homologue gene of *glut-2* in mammals, facilitated the release of glucose from intestinal cells to the interstitial fluid<sup>28</sup>. Research into how hyperglycemia affect the glucose and fat metabolism in *C. elegans* at gene level seems important.

In this study, the high-glucose condition was found to promote fat accumulation in transgenic worm VS29 (*hjSi56 vha-6p::GFP::dgat-2*), with the up-regulated expression of fat metabolism genes (*sbp-1*, *nhr-49*, and *fat-6*) and down-regulated expression of glucose metabolism gene *fgt-1*. The profound increase in *sbp-1*, *fat-6*, and *nhr-49* at the mRNA level indicated that high levels of glucose facilitated fat storage in worms as they do in mammals. It was also noted that the transport and consumption of glucose from intestinal cells may be disturbed after high-glucose treatment by down-regulation of *fgt-1*. Taken together, examination of the *sbp-1*, *nhr-49*, *fat-6*, and *fgt-1* genes is expected to elucidate their regulatory role and contribution to the treatment of diabetes, especially for patients with obesity. It is assumed that long term high-glucose conditions would promote the expression of oxidative stress protein GST-4 and disrupt the glucose transporter gene, which might be responsible for the fat storage and reduction in lifespan seen in worms. Because the insulin/insulin-like growth factor1 signaling pathway plays key roles in aging, development, dauer formation, and storage of

macronutrients in granules.<sup>54-58</sup> *C.elegans* shares the homology of the insulin/insulin-like growth factor 1 signaling pathway with humans; therefore, further studies to decipher the activation of this insulin/insulin-like growth factor 1 signaling pathway in regulating the lifespan reduction of worms subjected to excess glucose intake are needed.

## Conclusions

In summary, we present the worms-on-chip to resemble a diabetes-like model in vitro and to characterize multiple features of worms in response to high-glucose conditions. Hyperglycemia was found to shorten lifespan and increase oxidative stress and fat storage. The highly conserved nature of metabolism and genetics between worms and humans suggests that findings from *C. elegans* may contribute greatly to our understanding of diabetes in higher organisms. This device is capable of flexible operation with multiple functions, which not only supports the long-term single-worm culture with sufficient nutrient exchange, but also facilitates chemical stimuli and multi-parameter assay in a controllable and parallel manner, thus providing a new platform for the study of diabetes and drug testing in complications of diabetes and metabolism disorders.

## Acknowledgment

This research was supported by Key Laboratory of Separation Science for Analytical Chemistry (Dalian Institute of Chemical Physics, Chinese Academy of Sciences), International Science & Technology Cooperation Program of China (2015DFA00740), National Nature Science Foundation of China (Nos. 81273483, 81201689).

## Reference

1. P. S. Albert and D.L. Riddle, *Dev Biol*, 1988, 126, 270-293.
2. S. Hashmi, Y. Wang, R. S. Parhar, K. S. Collison, W. Conca, F. Al-Mohanna, R. Gaugler. *Nutr Metab (Lond)*, 2013, 10, 31-41.
3. S. Brenner, *Genetics of Caenorhabditis-Elegans*. *Genetics*, 1974, 77, 71-94.
4. J. R. Vanfleteren, B.P. Braeckman, *Neurobiology of Aging*, 1999, 20, 487-502.
5. J. J. Collins, K. Evason, and K. Kornfeld, *Exp Gerontol*, 2006, 41, 1032-1039.
6. C. D. Link, *Exp Gerontol*, 2006, 41, 1007-1013.
7. A. Schlotterer, G. Kukudov, F. Bozorgmehr, H. Hutter, X. L. Du, D. Oikonomou, Y. Ibrahim, F. Pfisterer, N. Rabbani, P. Thornalley, A. Sayed, T. Fleming, P. Humpert, V. Schwenger, M. Zeier, A. Hamann, D. Stern, M. Brownlee, A. Bierhaus, P. Nawroth, M. Morcos, *Diabetes*, 2009, 58, 2450-2456.
8. S. J. Lee, C.T. Murphy, C. Kenyon, *Cell Metab*, 2009, 10, 379-391.
9. M. Kumar, S. Nath, H. K. Prasad, G. D. Sharma, Y. Li, *Protein Cell*, 2012, 3, 726-738.
10. A. M. Garcia, M. L. Ladage, D. R. Dumesnil, K. Zaman, V. Shulaev, R. K. Azad, P. A. Padilla, *Genetics*, 2015, 200, 167-184.

11. M. Brownlee, *Nature*, 2001. 414, 813-820.
12. S. Nowaczewski, K. Stuper, T. Szablewski, H. Kontecka, *Poult Sci*, 2011, 90, 2467-2470.
13. A. Tauffenberger and J.A. Parker, *Plos Genetics*, 2014, 10(5), e1004346.
14. J.M. Olsen, M. Sato, O. S. Dallner, A. L. Sandstrom, D. F. Pisani, J. C. Chambard, E. Z. Amri, D. S. Hutchinson, T. Bengtsson, *J Cell Biol*, 2014, 207, 365-374.
15. J. Zheng and F.L. Greenway, *Int J Obes (Lond)*, 2012, 36, 186-194.
16. T. J. Schulz, K. Zarse, A. Voigt, N. Urban, M. Birringer, M. Ristow, *Cell Metabolism*, 2007, 6, 280-293.
17. S. Schmeisser, K. Zarse and M. Ristow, *Hormone and Metabolic Research*, 2011, 43, 687-692.
18. E. Wright, J.L. Scism-Bacon and L.C. Glass, *International Journal of Clinical Practice*, 2006, 60, 308-314.
19. G. P. Sykietis and D. Bohmann, *Science Signaling*, 2010. 3, re3
20. C. M. Felipe, A. N. Juliana, W. W. Hauswirth, R. Linden, P. S. Hilda, L. B. Chiarini, *Frontiers in Cellular Neuroscience*, 2015. 8, 438.
21. T. A. Staab, T. C. Griffen, C. Corcoran, O. Evgrafov, J. A. Knowles, D. Sieburth, *Plos Genetics*, 2013, 9(3), e1003354.
22. J. H. An and T.K. Blackwell, *Genes & Development*, 2003, 17, 1882-1893.
23. A. Weitzmann, C. Baldes, J. Dudek, R. Zimmermann, *Febs Journal*, 2007. 274, 5175-5187.
24. T. Nomura, M. Horikawa, S. Shimamura, T. Hashimoto, K. Sakamoto, *Genes Nutr*, 2010, 5, 17-27.
25. M. R. Van Gilst, H. Hadjivassiliou, A. Jolly, K. R. Yamamoto, *PLoS Biol*, 2005, 3, e53.
26. R. P. Gangwal, H. Hadjivassiliou, A. Jolly, K. R. Yamamoto, *Bioorg Med Chem Lett*, 2015, 25, 270-275.
27. T. J. Brock, J. Browse and J.L. Watts, *Plos Genetics*, 2006, 2, 997-1005.
28. K. Shun, A. D. Morielli, F. Q. Zhao, *Plos One*, 2013, 8, e68475.
29. H. Ma, L. Jiang, W. Shi, J. Qin, B. Lin, *Biomicrofluidics*, 2009, 3, 44114.
30. W. W. Shi, J. H. Qin, N. N. Ye, B. C. Lin, *Lab on a Chip*, 2008, 8, 1432-1435.
31. N. Kim, C. M. Dempsey, J. V. Zoval, J. Y. Sze, M. J. Madou, *Sensors and Actuators B-Chemical*, 2007, 122, 511-518.
32. K. H. Chung, M.M. Crane and H. Lu, *Nature Methods*, 2008, 5, 637-643.
33. M. M. Crane, J. N. Stirman, Chan-Yen Ou, P. T. Kurshan, J. M. Rehg, K. Shen, H. Lu, *Nature Methods*, 2012, 9, 977-980.
34. R. Siddique and N. Thakor, *Journal of the Royal Society Interface*, 2014, 11(90), 20130676.
35. S. E. Hulme, S. S. Shevkoplyas, A. P. McGuigan, J. Apfeld, W. Fontana, G. M. Whitesides, *Lab Chip*, 2010, 10, 589-597.
36. W. W. Shi, H. Wen, Y. Lu, Y. Shi, B. C. Lin, J. H. Qin, *Lab on a Chip*, 2010, 10, 855-2863.
37. P. Liu, R. J. Martin, L. Dong, *Lab Chip*, 2013, 13, 650-661
38. H. Wen, W. W. Shi and J. Qin, *Biomedical Microdevices*, 2012, 14, 721-728.

39. H. Wen, X. Gao and J. Qin, *Integrative Biology*, 2014, 6(1), 35-43.
40. H. Wen, Y. Yu, G. L. Zhu, L. Jiang, J. H. Qin, *Lab on a Chip*, 2015, 15, 1905-1911.
41. X.N. Ai, W. P. Zhuo, Q. L. Liang, P. T. McGrath and H Lu, *Lab Chip*, 2014, 14, 1746-1752
42. S. Johari, V. Nock, M.M. Alkaisi, W. H. Wang, *Lab Chip*, 2013, 13, 1699-1707
43. J. C. McDonald, D. C. Duffy, J. R. Anderson, D. T. Chiu, H. K. Wu, O. J. A. Schueller, G. M. Whitesides, *Electrophoresis*, 2000, 21, 27-40.
44. D. Qin, Y.N. Xia and G.M. Whitesides, *Advanced Materials*, 1996, 8, 917-919.
45. X. M. Zhao, Y.N. Xia and G.M. Whitesides, *Advanced Materials*, 1996, 8, 837-840.
46. S.R. Quake and A. Scherer, *Science*, 2000, 290, 1536-1540.
47. J. H. Qin and A.R. Wheeler, *Lab Chip*, 2007, 7, 186-192.
48. L. Kuerschner, C. Moessinger and C. Thiele, *Traffic*, 2008, 9, 338-352.
49. S. J. Stone, M. C. Levin, P. Zhou, J. Y. Han, T. C. Walther, R. V.Farese, *Journal of Biological Chemistry*, 2009, 284, 5352-5361.
50. P. J. McFie, S. L. Banman, S. Kary, S. J.Stone, *Journal of Biological Chemistry*, 2011, 286, 28235-28246.
51. T. Nguyen, P.J. Sherratt and C.B. Pickett, *Annual Review of Pharmacology and Toxicology*, 2003, 43, 233-260.
52. G.A. Otterson and F.J. Kaye, *Gene*, 1997, 199, 287-292.
53. M.P. Mayer and B. Bukau, *Cellular and Molecular Life Sciences*. 2005, 62, 670-684.
54. S. Ogg, S. Paradis, S. Gottlieb, G. I. Patterson, L. Lee, *Nature*, 1997, 389, 994-999.
55. T. Chiba, H. Yamaza and I. Shimokawa, *Current Genomics*, 2007, 8, 423-428.
56. J. A. Hanover, M. E. Forsythe, P. T. Hennessey, T. M. Brodigan, D. C. Love, G. Ashwell, M. Krause, *Proc Natl Acad Sci U S A*, 2005, 102, 11266-11271.
57. O. Stohr, K.Schilbach, L. Moll, M. M. Hettich, S. Freude, F. T. Wunderlich, M. Ernst, J. Zemva, J. C. Bruning, W. Krone, M. Udelhoven, M. Schubert, *Age*, 2013, 35, 83-101.
58. J. Zemva and M. Schubert, *Curr Diabetes Rev*, 2011, 7, 356-366.



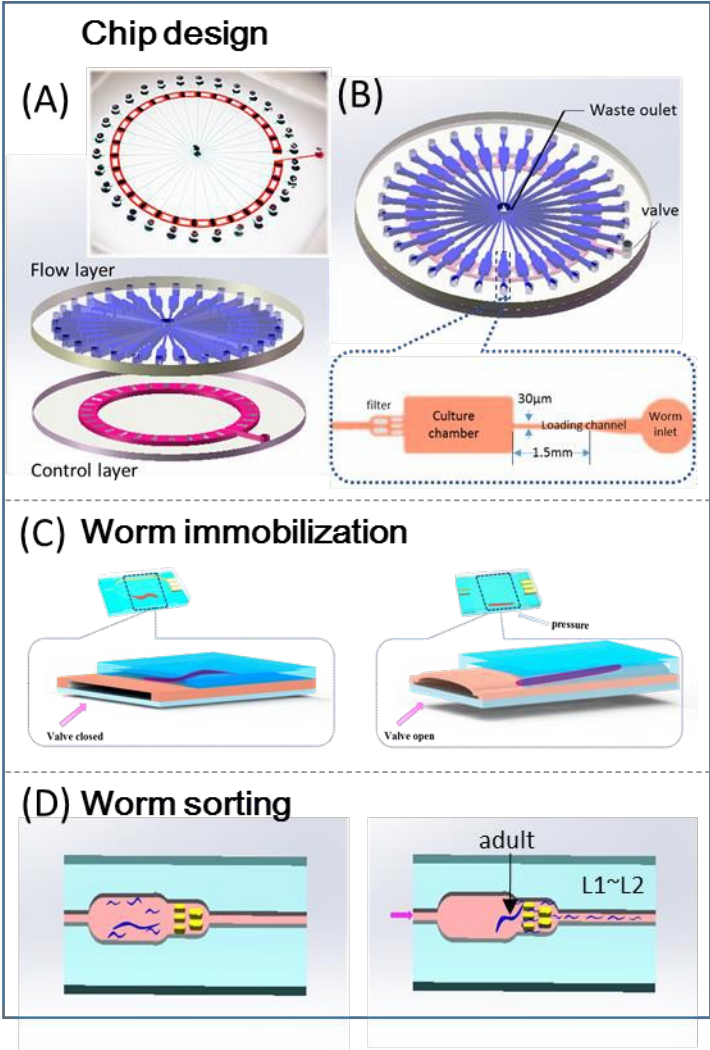


Fig.1. (A) Schematic and photograph of the microfluidic chip. The inset is a photograph of the fabricated microfluidic chip. (B) The magnified view of one unit. (C) Magnified illustration of the microvalve operation unit for worm loading and immobilization. (D) Schematic of worm screening in the chamber.

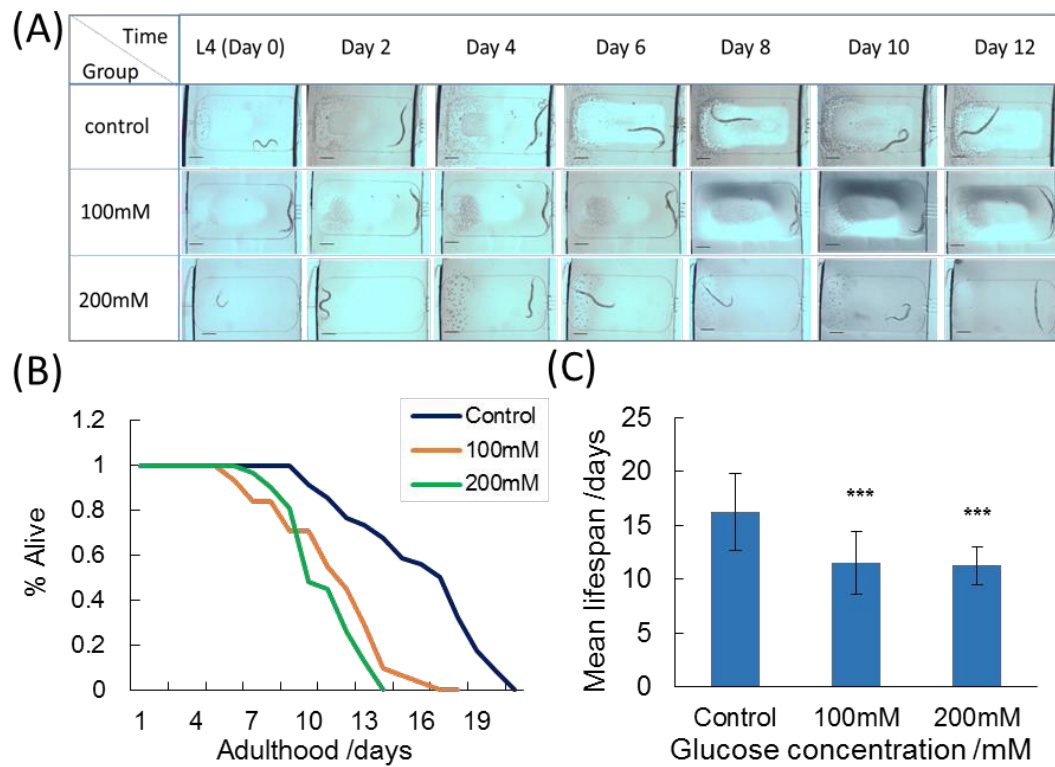


Fig.2. Characterization of the microfluidic device for lifespan analysis in worms. (A) Photographs of worms cultured on chip under different conditions. (B) Survival curves of worms. (C) The mean lifespan of worms in different groups. Scale bar=400  $\mu$ m. Error bars represent SEM ( $n \geq 30$ ). Error bars indicate the SEM relative to the control group. \*\*\* $p < 0.001$ .

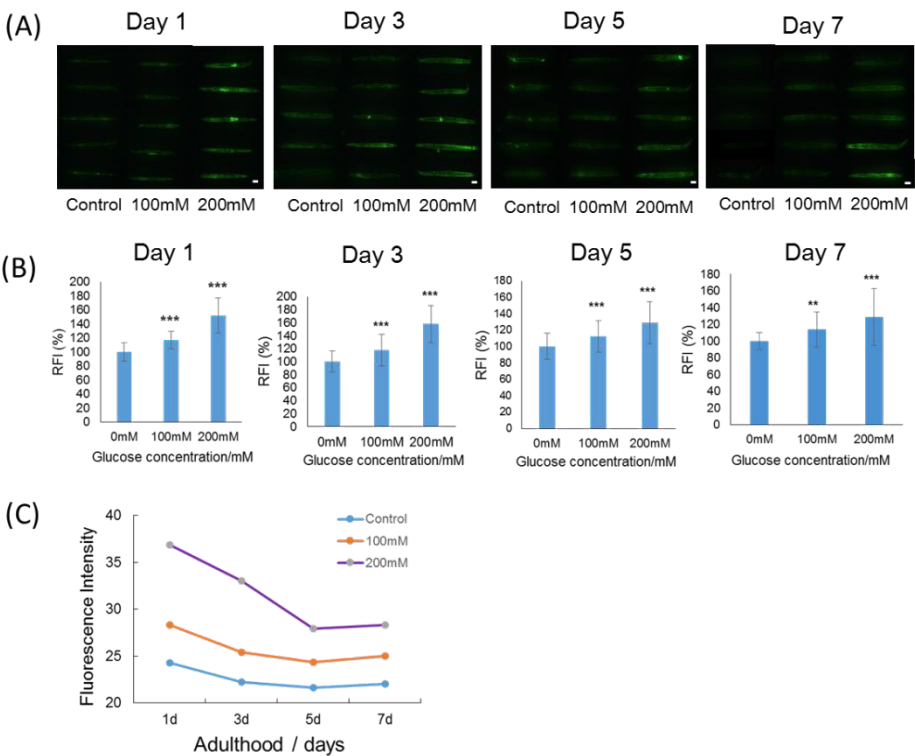


Fig.3. Comparisons of oxidative stress levels in adult CL2166 worms (*gst-4::GFP*) in response to various glucose concentrations. (A) Representative time-course images of *gst-4::GFP* expression in transgenic CL2166 worms treated with different glucose concentrations. Scale bar=100um. (B) Quantitative results of *gst-4::GFP* expression in CL2166 worms during the aging process. (C) The trend of *gst-4::GFP* expression in CL2166 worms under various glucose concentrations (0 mM, 100mM, and 200mM) during the aging process. Statistical analysis was conducted using Student's t-test. Error bars indicate the SEM ( $n \geq 30$ ) relative to day1 for the group with the same glucose condition. \*\* $p < 0.01$ , \*\*\* $p < 0.001$ .

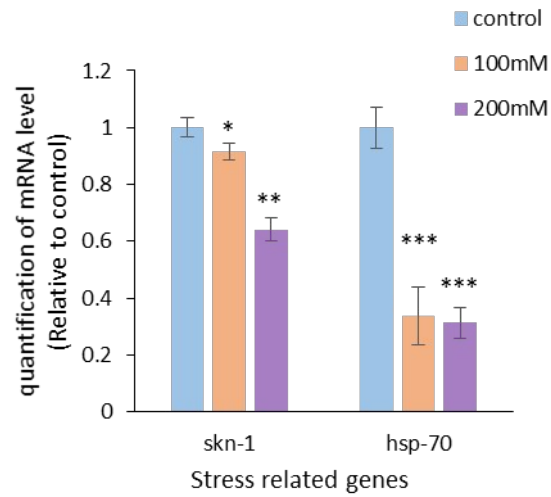


Fig.4. The effects of high glucose concentration on the expression of stress-related genes skn-1 and hsp-70 in worms using quantitative real-time PCR assay. The worms in different groups were treated with 100-mM and 200-mM glucose for 72 h ( $n \geq 300$ ). Error bars indicate the SEM relative to the control. \* $p < 0.05$ , \*\* $p < 0.01$ , \*\*\* $p < 0.001$ .

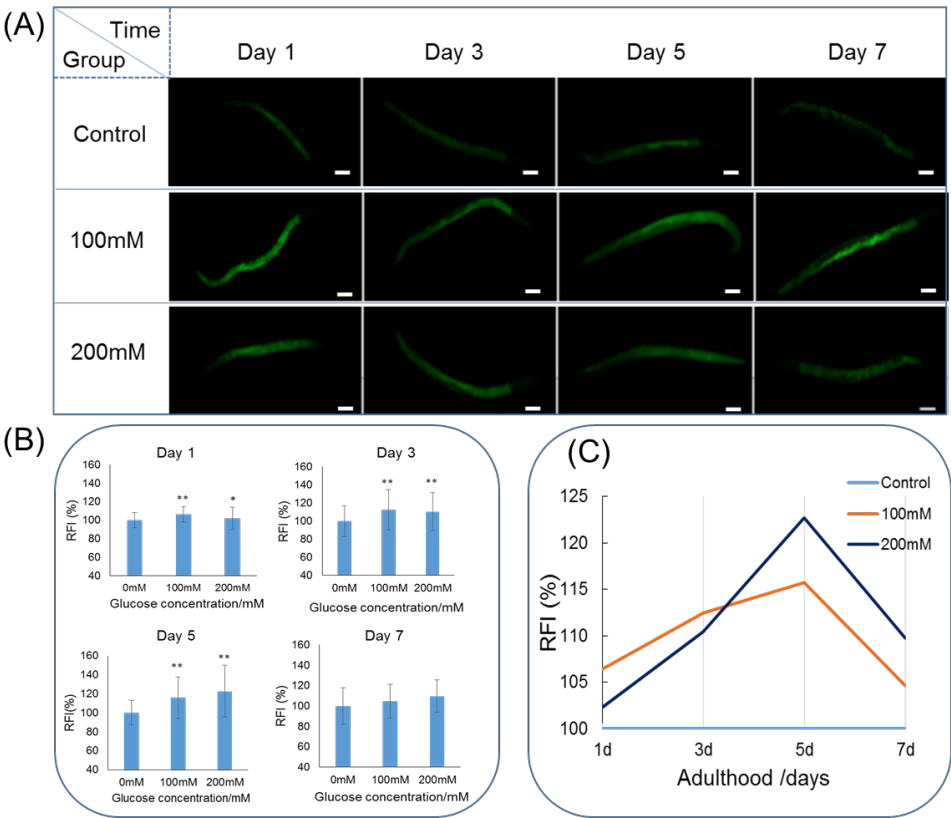


Fig.5 Comparison of fat accumulation in adult VS29 worms (GFP::dgat-2) in response to various glucose concentrations. (A) Representative time-course images of GFP::dgat-2 expression in transgenic VS29 worms treated with different glucose concentrations. Scale bar=100um. (B) Quantitative results of GFP::dgat-2 expression in VS29 worms during the aging process. (C) The trend of expression of GFP::dgat-2 in VS29 worms for glucose-treated worms compared to nontreated worms over 7 days. Statistical analysis was conducted using Student's t-test. Error bars indicate the SEM ( $n \geq 30$ ) relative to day1 for the group with the same glucose condition. \*\* $p < 0.01$ , \*\*\* $p < 0.001$ .



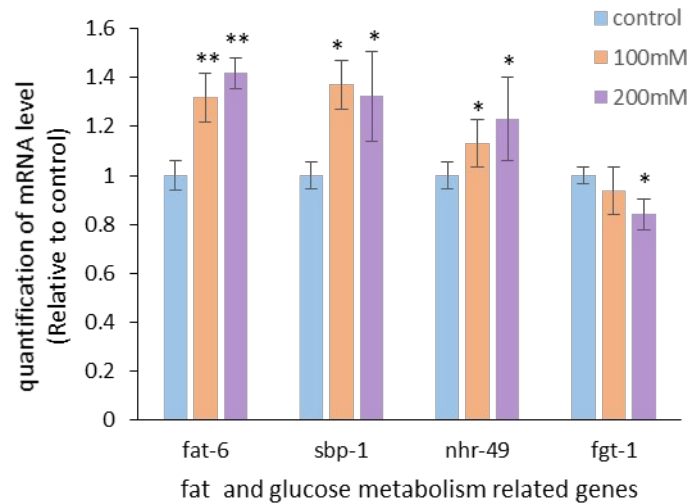


Fig.6. Characterization of the expression of glucose and lipid metabolism-associated genes (fat-6, sbp-1,nhr-49,fgt-1) in wild-type N2 worms subjected to excess glucose intake. The worms in different groups were treated with 0-mM, 100-mM,or 200-mM glucose for 72 h(n≥300). Error bars indicate the SEM relative to the control group. \*p<0.05, \*\*p<0.01.

Table 1. Primers for RT-PCR.

Primer Name	Sequence(from 5' to 3')
act-1-f	GTCATGGTTCGGTATGGGACA
act-1-r	AGTGAGGAGGACTGGGTGCT
fgt-1-f	GCATTCTCCGCATTTGTCAT
fgt-1-r	GGAAAGACCTCCAATCATAACCAC
nhr-49-f	GATTCGTGATGCTAGAAATCGTGT
nhr-49-r	ATCTTGTGGGTGCGTCATCT
sbp-1-f	AAGCAGTTGAGATTTGGGTC
sbp-1-r	GACGGTCATTGTCATTTAGGAT
fat-6-f	AAGGAACAAGGAGCCAAGC
fat-6-r	GGAAGAATGAAGCAGCACA
skn-1-f	AGTGTCGGCGTTCCAGAT
skn-1-r	AAGTGCGGGCAGCAACCT
hsp-70-f	AGAAGACGCAGCACAACG
hsp-70-r	TTCCATCCAACGAAGGGT

An microdevice to model type 2 diabetes–like hyperglycemia in *C.elegans* and examine several aspects of this disease in *C.elegans*.

